Aggregation of Melted DNA by Divalent Metal Ion-Mediated Cross-Linking

John G. Duguid and Victor A. Bloomfield
Department of Biochemistry, University of Minnesota, St. Paul, Minnesota 55108 USA

ABSTRACT In an accompanying paper we reported the use of differential scanning calorimetry and optical densitometry to characterize the melting and aggregation of 160 bp fragments of calf thymus DNA during heating in the presence of divalent metal cations. Aggregation is observed as thermal denaturation begins and becomes more extensive with increasing temperature until the melting temperature T_m is reached, after which the aggregates dissolve extensively. The order of effectiveness of the metals in inducing aggregation is generally consistent with their ability to induce melting: Cd > Ni > Co > Mn ≈ Ca > Mg. Under our experimental conditions (50 mg/ml DNA, 100 mM MCl_2, [metal]/[DNA phosphate] ≈ 0.6), no measurable aggregates were observed for BaDNA or SrDNA. In this paper we show that the Shibata-Schurr theory of aggregation in the thermal denaturation region provides a good model for our observations. Free energies of cross-linking, induced by the divalent cations, are estimated to be between 34% and 38% of the free energies of base stacking. The ability of a divalent metal cation to induce DNA aggregation can be attributed to its ability to disrupt DNA base pairing and simultaneously to link two different DNA sites.

INTRODUCTION

Divalent metal cations alter the stability of the DNA duplex. In general, the transition metals tend to destabilize DNA because they interact with the bases more extensively and disrupt base pairing (Eichhorn and Shin, 1968; Luck and Zimmer, 1972; Zimmer et al., 1974). The alkaline earth metals, however, stabilize DNA because they interact primarily with the phosphate groups and reduce the charge repulsion between opposing strands on the DNA double helix (Luck and Zimmer, 1972).

In addition to affecting DNA stability, divalent metal cations induce DNA aggregation at elevated temperatures. Knoll et al. (1988) showed that the ability of the divalent cations to induce DNA aggregation correlates strongly with their effectiveness in destabilizing DNA (Eichhorn and Shin, 1968). It was suggested that DNA aggregation could be the result of three possibilities: i) aggregation of fully denatured DNA, ii) aggregation of partially denatured DNA, or iii) aggregation of the intact duplex. Resolubilization of the aggregate, followed by treatment with S1 nuclease to detect single-strand DNA, showed that aggregation of fully denatured DNA was not likely. However, neither of the other two models was ruled out.

To obtain a better understanding of the connection between DNA melting and aggregation, we characterized these transitions using a combination of Raman spectroscopy, differential scanning calorimetry (DSC), optical densitometry, and pH potentiometry (Duguid et al., 1995). Concentrations were relatively high (55 mg/ml DNA, 100 mM MCl_2, [metal]/[DNA phosphate] ≈ 0.6) to give adequate signal/noise in the Raman and DSC experiments. We found that the metal-DNA complexes began to aggregate at or slightly below the detected onset of DNA melting, and the solutions became more turbid until the midpoint of the thermal melting transition (T_m) was reached. At temperatures between T_m and the completion of thermal denaturation, the turbidity decreased dramatically and the aggregates dissolved. No turbidity could be detected for DNA in the absence of divalent metal cations. These results suggest that DNA aggregation is best described by model ii), which requires the participation of partially melted regions in aggregation.

The mechanistic implication of this model is that the partially melted regions are cross-linked by divalent metal cations, and it is these cross-links that stabilize the aggregate. Shibata and Schurr (1981) developed a statistical mechanical theory of cross-linking of multistranded complexes to account for the increase in rotational relaxation time of DNA in the melting regime. In this study, we show that the Shibata-Schurr theory provides a plausible explanation of our melting and aggregation results, and enables extraction of thermodynamic parameters for cross-linking of DNA by divalent metal cations.

SHIBATA-SCHURR THEORY

For convenience, we present a brief outline of the Shibata-Schurr theory (Shibata and Schurr, 1981) of the cross-link-mediated aggregation of multistranded complexes. The original paper should be consulted for details. Consider for concreteness a four-stranded complex in which each strand is eight bases long (Fig. 1). Each of the four strands is linked to the others by base pairing interactions, represented by dark, thick lines that traverse the aggregate. Nine base pairs are shown in this particular configuration of the complex. The theory assumes that all of the strands are in register, so

Received for publication 12 October 1994 and in final form 31 August 1995.

Address reprint requests to Dr. Victor A. Bloomfield, Department of Biochemistry, University of Minnesota, 1479 Gortner Avenue, St. Paul, MN 55108. Tel.: 612-625-2268; Fax: 612-625-6775; E-mail: victor@molbio.cbs.umn.edu.

0006-3495/95/12/2642/07 $2.00

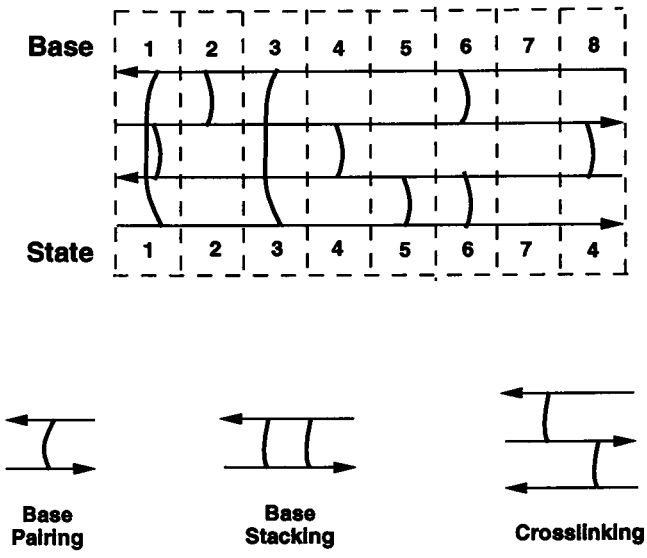

FIGURE 1 Diagram of a four-strand DNA complex, linked by base pairing interactions that are denoted by the cross-bars. Arrows associated with each DNA strand define the directionality. Numbers above the complex represent a particular site, and numbers below identify a particular state. In this illustration, there are a total of seven different possible states. The three different types of interactions that are observed within this configuration are shown below. Adapted from figure 1 of Shibata and Schurr (1981).

there is no sliding degeneracy. A dashed box encloses the bases that are aligned at each position in the aggregate. Each distinguishable arrangement of base pairs between the bases in the four strands in each of the eight dashed boxes represents a specific state. Fig. 1 shows the seven distinct states that can exist in the four-stranded complex. In general, the total number of distinct states ν_p that can occur at any site in a p-stranded DNA complex is

$$\nu_p = \sum_{k=0}^{p/2} \left\{ \frac{[(p/2)!]^2}{[(p/2-k)!]^2 k!} \right\} \tag{1}$$

where k is the number of base pairs at that site (dashed box).

In addition to base pairing interactions, there are two types of interactions between base pairs in neighboring sites. In double-stranded DNA, nearest-neighbor interactions occur between base pairs that share the same two strands. These are called stacked. However, in a multistranded complex such as that shown in Fig. 1, nearest-neighbor interactions may occur between base pairs that share either one or both strands. The latter is still considered a base stacking interaction, whereas the former is termed a cross-link. Cross-links can exist only in multistranded complexes. Fig. 1 shows only one stacking interaction, which occurs between the base pairs located at the bottom of sites 5 and 6. Four cross-linking interactions occur: two between sites 1 and 2, one between sites 2 and 3, and one between sites 4 and 5. Whereas base stacking causes a decrease in free energy under our experimental conditions, cross-linking is energetically unfavorable. The positive free energy of cross-linking is a barrier to the formation of multistrand complexes.

For a p-stranded complex containing n base pairs, a particular state j of the system can be described by a "microscopic" partition function $Q_{p,j,n}$ using the equation

$$Q_{p,j,n} = \exp\left(\frac{-n_j \Delta G_{BP}}{RT}\right) \exp\left(\frac{-m_j \Delta G_{BS}}{RT}\right) \exp\left(\frac{-r_j \Delta G_X}{RT}\right) \tag{2}$$

where ΔG_{BP}, ΔG_{BS}, and ΔG_X are the free energies of base pairing, base stacking, and cross-linking; and n_j, m_j, and r_j are the number of base pairing, stacking, and cross-linking interactions. In Fig. 1, $n_j = 9$, $m_j = 1$, and $r_j = 4$. Assuming that the enthalpy of melting is completely dominated by base stacking, the free energy of base pairing can be defined by the equation

$$\Delta G_{BP} = -RT \ln \sigma \tag{3}$$

where σ is the helix initiation or cooperativity parameter. The free energy of base stacking is defined by the equation

$$\Delta G_{BS} = T(\Delta S_{cal} + R \ln \sigma) - \Delta H_{cal} \tag{4}$$

where ΔH_{cal} and ΔS_{cal} are the melting enthalpy and entropy per base pair measured by DSC. The free energy of cross-linking (ΔG_X) is treated as an adjustable parameter to fit the calculations from the Shibata-Schurr theory to experimentally determined aggregation profiles.

We see that determination of ΔG_{BP} and ΔG_{BS} requires four parameters: ΔH_{cal}, ΔS_{cal}, T_m (which is required indirectly), and σ. The first three can be determined from DSC, whereas σ requires a combination of DSC and helix-coil transition theory (Cantor and Schimmel, 1980). Once these parameters are obtained, $Q_{p,j,n}$ is calculated as a function of temperature. $Q_{p,j,n}$ represents a particular configuration of the system in which a particular order of base pairing occurs. To characterize the entire system of the p-stranded complex containing n base pairs, $Q_{p,j,n}$ must be summed over all possible configurations to obtain the partition function

$$K_{p,n} = \sum_{j_1=1}^{\nu_p} \cdots \sum_{j_N=1}^{\nu_p} Q_j \tag{5}$$

If one assigns the single-stranded species as the standard state, $K_{p,n}$ also represents an equilibrium constant between the single strands and the p-stranded complex:

$$p m_1 \overset{K_p}{\rightleftarrows} m_p \tag{6}$$

This formulation can be expressed in the equation

$$K_{p,n} = \frac{m_p}{m_1^p} \tag{7}$$

where m_p is the concentration of p-strands in solution and m_1 is the concentration of single strands. Combining the

conservation law for the total concentration of single strands, $m_{1,tot}$,

$$\sum_{p=1}^{p_{max}} pm_p = m_{1,tot} \quad (8)$$

with Eq. 7, we obtain

$$\sum_{p=1}^{p_{max}} pm_1^p K_p = m_{1,tot} \quad (9)$$

where p_{max} is the maximum strandedness that is computationally practical. According to Eq. 1, ν_p increases very rapidly, from 7 with $p = 4$, to 34 with $p = 6$, to 209 with $p = 8$. We used $p_{max} = 6$ for all of the calculations reported here.

Equation 9 represents a polynomial equation of order p_{max} that can be solved iteratively for m_1. The values of m_1, and K_p obtained from Eq. 5, are entered into Eq. 7 to determine m_p. The result is a temperature-dependent profile of the concentration of p-stranded complexes, which can be determined for $p = 1$ to p_{max}. From these calculations, two important quantities are obtained: the average number of strands in a complex at a given temperature, $\bar{p}$, and the average number of base pairs in the p-stranded complex, $\bar{n}_{BP}$. The former is determined from the equation

$$\bar{p} = \sum_{p=1}^{p_{max}} pm_p \Big/ \sum_{p=1}^{p_{max}} m_p \quad (10)$$

and the latter from

$$\bar{n}_p = \partial \ln(K_p)/\partial(-\Delta G_{BP}/RT) \quad (11)$$

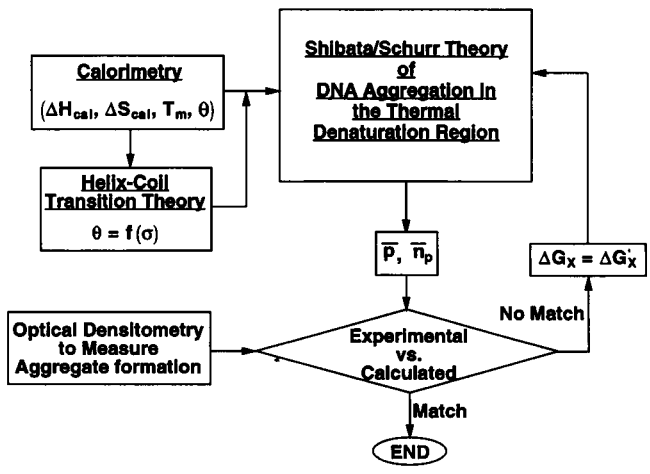

FIGURE 2 Flow chart illustrating the relationship between experimental and theoretical design for measuring DNA aggregation in the presence of divalent metal cations. Initially, thermodynamic parameters are incorporated into the Shibata-Schurr theory, which generates aggregation ($\bar{p}$) and melting ($\bar{n}p$) profiles. Comparison is made between and the turbidity profile obtained by optical densitometry. ΔG_X is then adjusted iteratively until the two profiles match.

TABLE 1 Thermodynamic parameters for the melting of DNA-metal complexes

Sample	ΔH_{cal} (kcal)	ΔS_{cal} (cal/°K)	T_m (°C)	σ ($\times 10^3$)
CdDNA	6.8	21.0	51.8	5.8
NiDNA	6.7	19.9	62.5	1.9
CoDNA	7.3	21.4	67.8	2.2
MnDNA	8.6	24.5	77.2	10.3
CaDNA	8.7	24.7	79.2	4.1
MgDNA	7.8	21.9	83.6	4.6
BaDNA	6.2	17.5	81.2	3.5
SrDNA	7.3	20.6	83.5	4.6
DNA	6.7	19.3	75.5	10.9

Data from Duguid et al. (1995).

Equations 10 and 11 are the basis for calculating the aggregation and melting profiles, which are to be compared with experimental observations. Equation 11 was normalized between 0 and 160 bp of double-stranded DNA to yield $\bar{n}_{BP}$. It should be noted that the number of base pairs formed according to Eq. 11 is not the same as that determined from a standard thermal melting experiment in dilute solution,

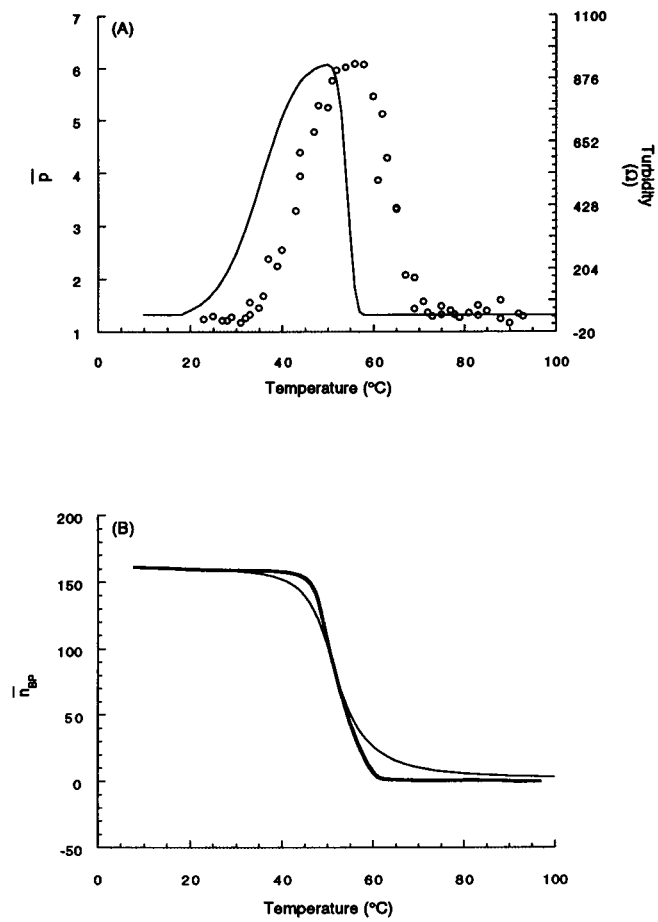

FIGURE 3 Aggregation and melting profiles of CdDNA. (*A*) Aggregation. Circles and right axis, experimental; solid line and left axis, calculated. (*B*) Melting. Light line, experimental; heavy line, calculated.

because Eq. 11 includes base pairs formed by cross-linking. However, the difference is not very large.

The process of adjusting ΔG_X to obtain $\bar{p}$ and $\bar{n}_{BP}$ as best fits to the experimental aggregation and melting profiles is diagrammed in the flow chart of Fig. 2. To start out, DSC was used to calculate ΔH_{cal}, ΔS_{cal}, T_m, and the helix fraction θ as a function of T for the melting of the metal-DNA complexes. Structural changes accompanying melting were confirmed by Raman spectroscopy (Duguid et al., 1995). In the same paper, helix-coil transition theory was used in combination with θ to evaluate σ (Cantor and Schimmel, 1980). ΔH_{cal}, ΔS_{cal}, and σ were then entered into the equations for ΔG_{BP} and ΔG_{BS}. An initial guess of ΔG_X was made and $\bar{p}$ and $\bar{n}_{BP}$ were determined using the Shibata-Schurr theory. ΔG_X was adjusted iteratively until the best fit (judged by eye) was obtained between $\bar{p}$ and the aggregation profile obtained from optical densitometry.

RESULTS

Table 1 shows the melting parameters of the metal-DNA complexes, obtained by DSC and helix-coil transition theory (Duguid et al., 1995). ΔH_{cal} and ΔS_{cal} are in the same range as those obtained by previous studies (Breslauer et al., 1986). The variation among ΔH_{cal} and ΔS_{cal} may be attributed in part to the different affinities of the divalent metals for DNA, and in part to differences in hydration of the DNA sample when it is weighed. The T_m values show that Cd, Ni, and Co destabilize the double helix, whereas Mn, Ca, Mg, Ba, and Sr stabilize it. This is expected because transition metals have higher affinities for the bases and induce a relative destabilization of base pairing interactions. The nucleation parameter, σ, varies between 10^{-3} and 10^{-2} and is smaller for the metal-DNA complexes than for DNA without metal (Duguid et al., manuscript in preparation). This effect has been attributed to an enhanced cooperativity of melting at higher ionic strength (Dove and Davidson, 1962; Record et al., 1978). We also note that σ is larger for this random-sequence calf thymus DNA than it would be for a homopolynucleotide, because the observed breadth of the transition reflects sequence and base composition heterogeneity as well as base stacking cooperativity.

Comparisons between calculated and experimental profiles of aggregation and melting are shown for each of the metal-DNA complexes in Figs. 3-8. Two samples, BaDNA

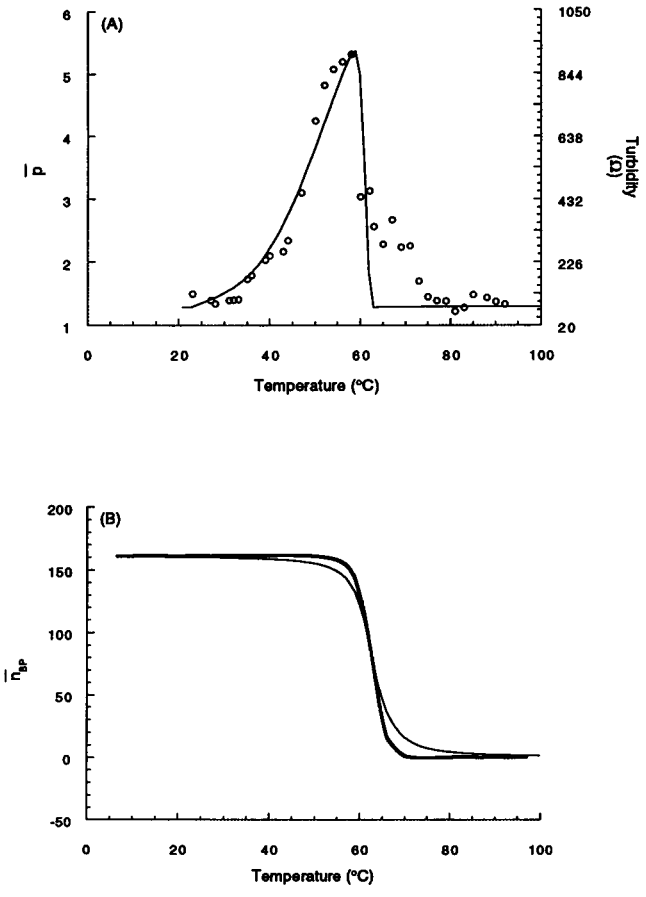

FIGURE 4 Aggregation and melting profiles of NiDNA. (*A*) Aggregation. Circles and right axis, experimental; solid line and left axis, calculated. (*B*) Melting. Light line, experimental; heavy line, calculated.

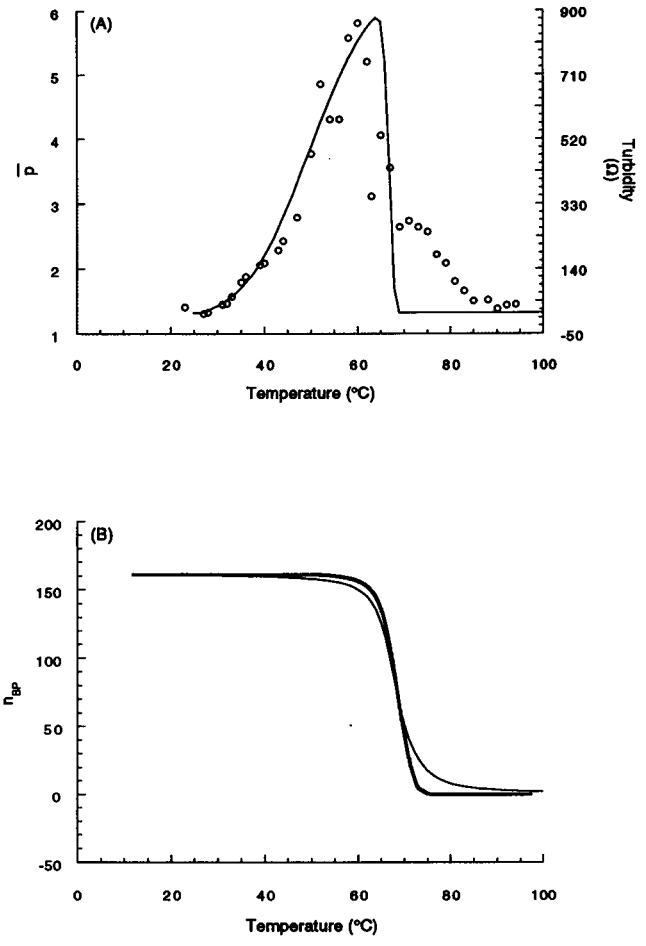

FIGURE 5 Aggregation and melting profiles of CoDNA. (*A*) Aggregation. Circles and right axis, experimental; solid line and left axis, calculated. (*B*) Melting. Light line, experimental; heavy line, calculated.

and SrDNA, did not aggregate under our experimental conditions, so their profiles are not given. The profiles were calculated from Eqs. 10 and 11 after iterative determination of the parameters in Tables 1 and 2. Agreement of the calculated and observed $\bar{n}_{BP}$ versus T is generally quite good, although the calculated curves are all somewhat sharper than the experimental ones. We attribute this mainly to the assumption that all of the enthalpy of melting comes from base unstacking. Although this is a good approximation, calculations (J. Duguid, unpublished observations) show that the sharpness of the calculated melting transition can be controlled by partitioning the total enthalpy between base unstacking and unpairing. Also, as noted above and explored further at the end of this section, the compositional and sequence heterogeneity of the DNA should have some effect on the shape of the transition.

The calculated $\bar{p}$ versus T curves were generally in good agreement with the turbidimetric measurement of aggregation (Duguid et al., 1995). For Ni, Co, Ca, and Mg, we observed a substantial decrease in turbidity very near T_m, as predicted by the Shibata-Schurr theory. Multistranded DNA complexes cannot maintain their integrity much above T_m.

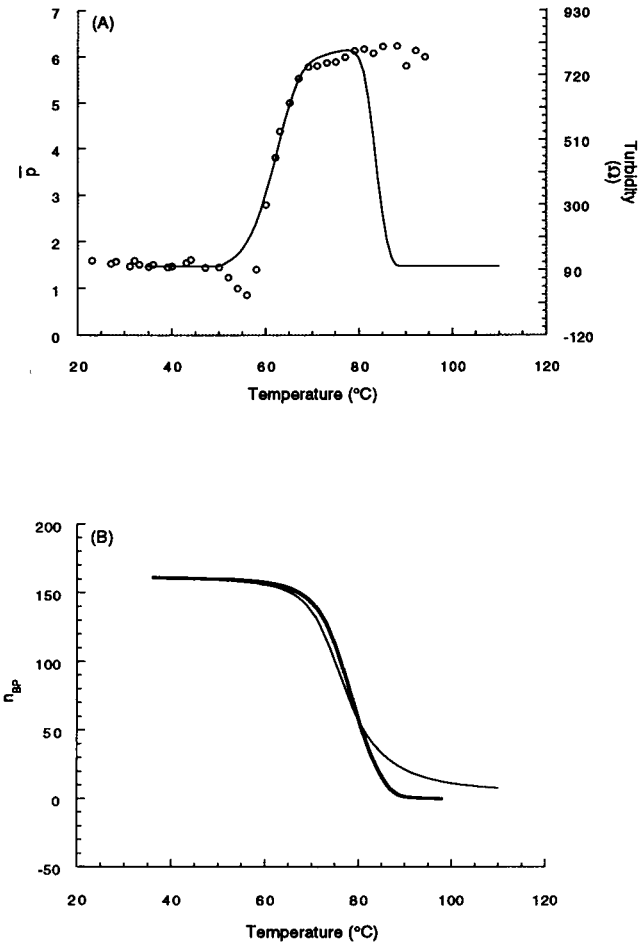

FIGURE 6 Aggregation and melting profiles of MnDNA. (*A*) Aggregation. Circles and right axis, experimental; solid line and left axis, calculated. (*B*) Melting. Light line, experimental; heavy line, calculated.

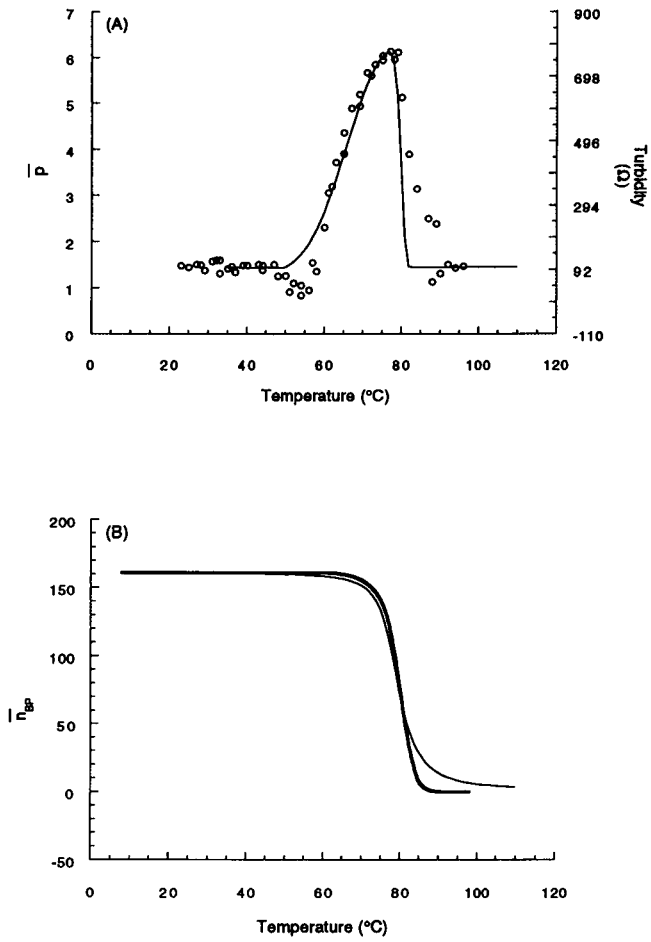

FIGURE 7 Aggregation and melting profiles of CaDNA. (*A*) Aggregation. Circles and right axis, experimental; solid line and left axis, calculated. (*B*) Melting. Light line, experimental; heavy line, calculated.

For unknown reasons, the theoretical transition curve for Cd is displaced a few degrees below experimental. As seen in Fig. 6, MnDNA was the only complex that did not disaggregate at temperatures above T_m, even up to 100°C. Apparently, cross-linking mediated by Mn is very stable once DNA melting is initiated. Currently, there is no evidence to indicate that Mn cross-links different sites than the other divalent metals. In general, however, Figs. 3–8 suggest that the mechanism of DNA aggregation is the same for most of the transition and alkaline earth metals.

By fitting experimental and theoretical aggregation profiles, we were able to estimate the free energies of cross-linking, ΔG_X, induced by each of the divalent metal cations. These are shown in Table 2, expressed as fractions of the free energies of base stacking, ΔG_{BS}. ΔG_X lies within a narrow range between 34 and 38% of ΔG_{BS} for all of these complexes. There appears to be a trend that $\Delta G_X/\Delta G_{BS}$ increases slightly with the breadth of the aggregation transition. Large changes in the width of the aggregation curve results arise from small changes in ΔG_X. This is seen clearly in Fig. 9, where it is also seen that the cross-linking free

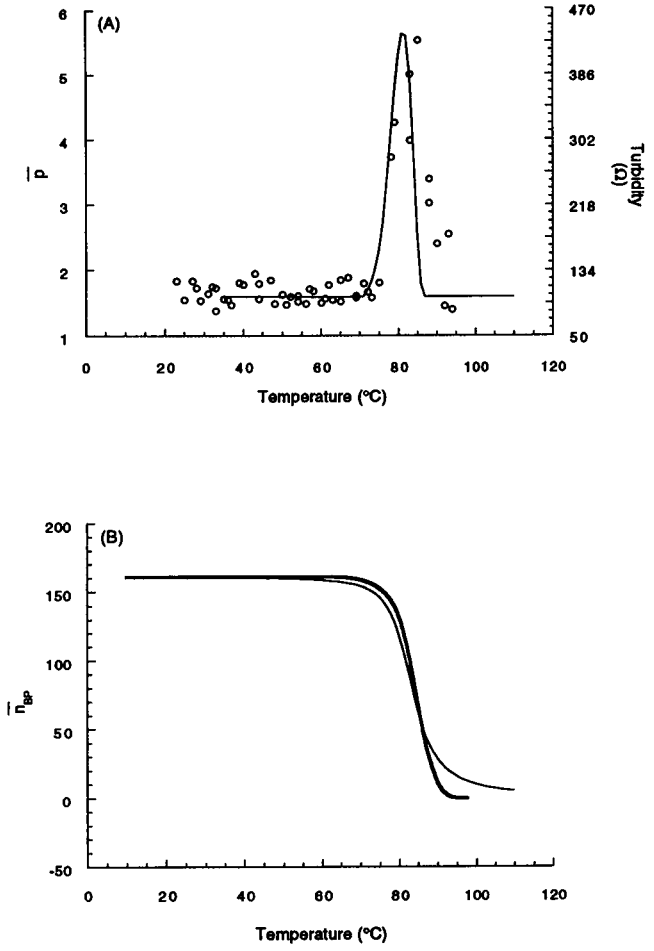

FIGURE 8 Aggregation and melting profiles of MgDNA. (*A*) Aggregation. Circles and right axis, experimental; solid line and left axis, calculated. (*B*) Melting. Light line, experimental; heavy line, calculated.

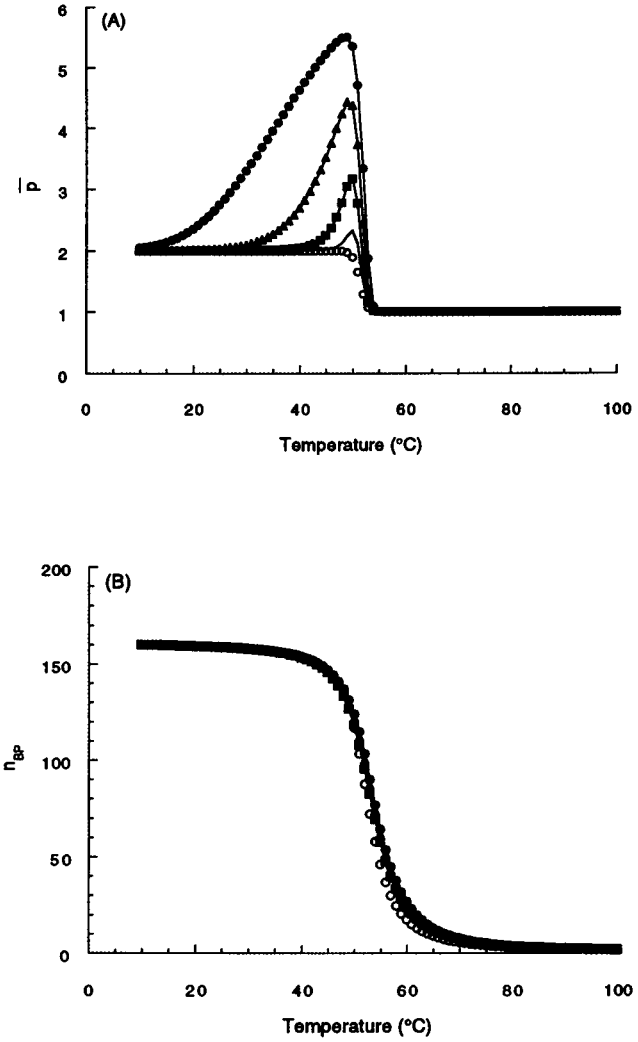

FIGURE 9 Calculated effect of lowering cross-linking free energy ΔG_x on the (*A*) aggregation and (*B*) melting profiles of NiDNA. ○, $\Delta G_x = -\Delta G_{BS}$; —, $\Delta G_x = 0.35\ \Delta G_{BS}$; ■, $\Delta G_x = 0.36\ \Delta G_{BS}$; ▲, $\Delta G_x = 0.37\ \Delta G_{BS}$; ●, $\Delta G_x = 0.38\ \Delta G_{BS}$.

energy affects only slightly the dependence of $\bar{n}_{BP}$ on temperature.

As noted above, the value of σ derived from the DSC curves and used in our calculations is artificially high, because of the sequence and compositional heterogeneity of the sample. To explore the effect of this approximation, we have analyzed the NiDNA transition as the sum of three curves separated by 2 K in T_m and with different σ and ΔH_{cal}, chosen to reproduce the thermal melting curve. The values for σ, T_m/K, and ΔH_{cal}/kcal/mol bp for the three curves are 1.2×10^{-3}, 333.65, 6.65; 8.5×10^{-4}, 335.65, 6.69; and 7×10^{-4}, 337.65, 6.73. These are to be compared with the values in Table 1 (1.9×10^{-3}, 335.65, 6.69) obtained as the best fit to a single set of transition parameters. In all cases the transition entropy was maintained at 19.9 cal/K-mol bp. The values of ΔG_X derived from this analysis range from $0.37\Delta G_{BS}$ to $0.40\Delta G_{BS}$. This is very close to the value $0.38\Delta G_{BS}$ obtained for the single transition, indicating that estimates of the cross-linking free energy are relatively insensitive to the details of the transition.

TABLE 2 Aggregation parameters for DNA-metal complexes

Sample	$\Delta G_X/\Delta G_{BS}$	$T_{a,calc}$ (°C)	$T_{a,exp}$ (°C)
CdDNA	0.360	49.8	55.4
NiDNA	0.380	58.8	58.3
CoDNA	0.383	63.6	60.3
MnDNA	0.340	76.7	—
CaDNA	0.368	76.4	76.4
MgDNA	0.340	81.2	84.9
BaDNA	—	—	—
SrDNA	—	—	—
DNA	—	—	—

DISCUSSION

In previous work we proposed that DNA aggregation in the presence of divalent metal cations is probably due to the interaction of partially melted regions on different strands

(Knoll et al., 1988) and showed that the structural distortions induced in the double helix by transition metal ions are consistent with this explanation (Duguid et al., 1995). In this paper, we have shown that the Shibata-Schurr (1981) theory of multistrand aggregation in the thermal denaturation region accounts quantitatively for our observations, with a free energy of cross-linking that seems physically reasonable. The aggregation is driven both by the thermal separation of the strands of the duplex, a process that is primarily enthalpic, and by the formation of cross-links, which has a large entropic component because of the very large number of microstates that can exist in multistranded complexes. Shibata and Schurr have pointed out that the aggregation transition should be strongly molecular-weight dependent, because the number of microstates is a power function of the number of base pairs. We may have seen some evidence of this effect in our Raman spectroscopic study of DNA in the presence of divalent metals (Duguid et al., 1993), where high-molecular-weight calf thymus DNA, but not 160 bp fragments, showed turbidity even at room temperature and below.

Our formulation of the cross-linking thermodynamics allows no explicit role for the divalent metal cations. The cation concentration, and its binding to the separated and cross-linked nucleotides, are all absorbed in the single parameter ΔG_X. Addition of divalent metal lowers ΔG_X from the presumably positive or only slightly negative value characteristic of DNA in the absence of metal, to a negative value about 34–38% of G_{BS}. This large negative value of ΔG_X is required for stabilization of multistranded cross-links. It remains for future work to develop a detailed structural picture of bases and metal ions in the cross-linked state, and thereby to understand the origins of this strongly stabilizing free energy.

We are grateful for useful discussions with Prof. J. M. Schurr (University of Washington). We also acknowledge Profs. G. J. Thomas, Jr., and J. M. Benevides (University of Missouri-Kansas City) for their collaboration on laser Raman studies of the metal-DNA complexes.

This research was supported by National Institutes of Health grant GM28093 to V.A.B. and by a Molecular Biophysics Predoctoral Traineeship from National Institutes of Health (GM08277) to J.G.D.

REFERENCES

Breslauer, K. J., R. Frank, H. Blocker, and L. A. Marker. 1986. Predicting DNA duplex stability from the base sequence. *Proc. Natl. Acad. Sci. USA.* 83:3746–3750.

Cantor, C. R., and P. R. Schimmel. 1980. Biophysical Chemistry. Part III. The Behavior of Biological Macromolecules. W. H. Freeman and Co., San Francisco.

Dove, W. F., and N. Davidson. 1962. Cation effects on the denaturation of DNA. *J. Mol. Biol.* 5:467–478.

Duguid, J., V. Bloomfield, J. Benevides, and G. Thomas, Jr. 1993. Raman spectroscopy of DNA-metal complexes. I. Interactions and conformational effects of the divalent cations: Mg, Ca, Sr, Ba, Mn, Co, Ni, Cu, Pd, and Cd. *Biophys J.* 65:1916–1928.

Duguid, J., V. A. Bloomfield, J. M. Benevides, and G. J. Thomas, Jr. 1995. Raman spectroscopy of DNA-metal complexes. II. The thermal denaturation of DNA in the presence of Sr^{2+}, Ba^{2+}, Mg^{2+}, Ca^{2+}, Mn^{2+}, Co^{2+}, Ni^{2+}, and Cd^{2+}. *Biophys. J.* 69:2614–2632.

Eichhorn, G. L., and Y. A. Shin. 1968. Interaction of metal ions with polynucleotides and related compounds. XII. The relative effect of various metal ions on DNA helicity. *J. Am. Chem. Soc.* 90:7323–7328.

Knoll, D. A., M. G. Fried, and V. A. Bloomfield. 1988. Heat-induced DNA aggregation in the presence of divalent metal salts. *In* Structure and Expression: DNA and Its Drug Complexes. Adenine Press, Albany.

Luck, G., and C. Zimmer. 1972. Conformational aspects and reactivity of DNA: effects of manganese and magnesium ions on interaction with DNA. *Eur. J. Biochem.* 29:528–536.

Record, M. T., Jr., C. F. Anderson, and T. M. Lohman. 1978. Thermodynamic analysis of ion effects on the binding and conformational equilibria of proteins and nucleic acids: the roles of ion association or release, screening, and ion effects on water activity. *Q. Rev. Biophys.* 11:103–178.

Shibata, J. H., and J. M. Schurr. 1981. A theory of aggregation in the thermal denaturation region of multistrand biopolymers. *Biopolymers.* 20:525–549.

Zimmer, C., G. Luck, and H. Triebel. 1974. Conformation and reactivity of DNA. IV. Base binding ability of transition metal ions to native DNA and effect on helix conformation with special reference to DNA-Zn(II) complex. *Biopolymers.* 13:425–453.